

Short-lived radionuclides (^7Be and ^{210}Pb) as tracers of particle dynamics in a river system in southeast Michigan

Jason Jweda, Mark Baskaran, and Ed van Hees

Department of Geology, Wayne State University, Detroit, Michigan 48202

Linda Schweitzer

Chemistry Department, Oakland University, Rochester, Michigan 48309

Abstract

Riverine water samples (dissolved and particulate), surficial bottom sediments, and trapped sediments were collected mostly monthly from three stations along the Clinton River, in southeastern Michigan, over a period of ~ 1 yr and analyzed for ^7Be and ^{210}Pb to elucidate the types and rates of processes affecting particle dynamics in a riverine system. Using a simple irreversible scavenging box model approach, sources and sinks for dissolved and particulate ^7Be and ^{210}Pb were quantified to estimate their residence times in the dissolved and particulate phases. Resuspension rates of surficial bottom sediments calculated from the mass balance of particulate ^7Be varied from 0.50 to 1.34 (geometric mean: 0.83 ± 0.34 g cm^{-2} yr^{-1}), while corresponding values varied from 0.16 to 1.48 (GM: 0.38 ± 0.38 g cm^{-2} yr^{-1}) using particulate ^{210}Pb . Based on the ^{210}Pb mass balance, it appears that only $\sim 2\%$ of ^{210}Pb was derived from direct atmospheric deposition, while $\sim 98\%$ was derived from resuspension of bottom sediments. Additionally, there was a large discrepancy between mass flux collected in the trap (GM: 8.9 g cm^{-2} yr^{-1}) compared to net sediment accumulation rates (GM: 0.88 ± 0.38 g cm^{-2} yr^{-1}), which was attributed to sediment resuspension; this may provide insight into the frequency of particle-recycling events. Furthermore, desorption of particle-reactive species during resuspension events could result in the mobility of contaminants to farther distances from the contaminated site. Therefore, this study has direct relevance to the uptake of particle-reactive species in a riverine system and thereby the water quality of rivers.

The partitioning of naturally occurring, particle-reactive radionuclides between the particulate and dissolved phases has provided insight on the biogeochemical cycling of particulate matter as well as particle-reactive elements in freshwater systems. Rivers are the major conduits to lakes or oceans, and hence biogeochemical cycling of particle-reactive species (including organic and inorganic contaminants) in rivers will have an impact on the water quality of lakes. Particle-reactive radionuclides, such as ^7Be and ^{210}Pb , have been extensively utilized in coastal systems as proxies for contaminants and tracers of particle dynamics because direct study of the transport, deposition, and resuspension of particle-reactive species is difficult. The radionuclides ^7Be (half-life [$T_{1/2}$] = 53.3 d), which is a cosmogenic radionuclide primarily produced in the atmosphere, and ^{210}Pb ($T_{1/2}$ = 22.3 yr), which is ultimately produced from the radioactive decay of ^{222}Rn , are both scavenged by precipitation and aerosols in the atmosphere and subsequently deposited on Earth's surface. Following atmospheric deposition into surface waters, ^7Be and ^{210}Pb are scavenged by adsorption onto particulate matter in the water column. Particle scavenging, therefore, is an important "self cleaning" mechanism that scrubs aqueous

systems of particle-reactive substances such as trace metals, organic contaminants, and radionuclides (e.g., Broecker et al. 1973; Bacon et al. 1976; Baskaran and Santschi 1993).

Although there have been several studies using ^7Be and ^{210}Pb as particle and contaminant tracers in the marine environment, relatively few studies in freshwater systems, including rivers, have been conducted (e.g., Benoit and Hemond 1987; Balistrieri et al. 1995; Chai and Urban 2004). The Clinton River watershed is an ideal study site because the sediments are contaminated with heavy metals and organic pollutants such as polychlorinated biphenyls (PCBs) as a result of industrialization and urbanization (USEPA 2006). The pollution from rivers discharging into Lake St. Clair is of great concern because approximately one third of the Great Lakes fish caught and the drinking water for ~ 4.5 million people come from this lake.

The primary objective of this study was to investigate the partitioning of two particle-reactive radionuclides between solution and particulate phases in a riverine system. From this partitioning study, we answer the following key questions: (1) What are the residence times and removal rates of ^7Be and ^{210}Pb from the riverine water column? (2) Can sediment resuspension rates be modeled and quantified using a ^7Be and ^{210}Pb mass balance approach in a riverine system? (3) How much of the particle-bound ^{210}Pb is recycled, and can we quantify the resuspended ^{210}Pb and atmospherically derived contribution in the sediment? (4) What are the distribution coefficients of ^7Be and ^{210}Pb ? (5) How do the affinities of ^7Be and ^{210}Pb for particulate matter differ in a riverine system? Answers to these questions may provide valuable insight into the fate and transport of

Acknowledgments

This study was funded in part by a grant from the U.S. Environmental Protection Agency. We thank the two anonymous reviewers and the associate editor for their constructive reviews of this manuscript. The results presented in this paper are a part of a Master's thesis submitted to the Department of Geology, Wayne State University (J.J.).

contaminants that have similar particle reactivities (such as PCBs) in riverine systems (e.g., Fitzgerald et al. 2001). The extent and frequency of recycling of particulate matter from bottom sediments have an effect on the sorption–desorption of particle-reactive contaminants, thereby affecting the water quality in the river and ultimately the lake where the river discharges.

Materials and methods

The study area—The Clinton River, located in south-eastern Michigan (Fig. 1), drains ~ 1980 km² of the northern suburbs of Detroit, including a portion of four different counties (Macomb, Oakland, St. Clair, and Lapeer). The main branch of the Clinton River is 127 km long, an average of 53.6 m wide, and contains 418 km of major tributaries (Francis and Haas 2005). The north and main branches converge to form the lower Clinton River where all sampling sites were located. The average annual flow rate at the most downstream U.S. Geological Survey (USGS) gauge station on the main branch is 21.5 m³ s⁻¹ (USGS 2006). The Clinton River empties into Lake St. Clair, where it forms a small delta composed of the Clinton River mouth, a spillway. Lake St. Clair is a small (1114 km²) shallow (3.6-m mean depth) body of water in the Great Lakes system that is part of the connecting channel between Lake Erie and Lake Huron. The hydrogeology of the watershed is primarily controlled by glacial deposits; moraines and outwash plains occur in the western portion, and ancient lake deposits occur in the eastern portion (Francis and Haas 2005).

Field sampling—Water, bottom sediments, and sediment trap samples were collected mostly monthly from September

2004 to August 2005 from three sampling stations along the river (Fig. 1). Station locations and analyses performed are given in Table 1. At each station, a sediment trap assemblage consisting of two individual trap tubes was deployed over the duration of the sampling period (7–46 d, except 3 samples; Table 2). The sediment trap was modified from a design by Marvin et al. (2004). Briefly, sediment traps consisted of two polypropylene core tubes, 100 cm in length and 9.5 cm in diameter. Teflon cups were attached to the bottom end of each tube to collect settling sedimentary particles. A concrete-filled tire weighing ~ 63 kg served as an anchor for the sediment trap assemblage. The small aspect ratio (diameter:length = 0.095:1) aided to prevent settled suspended sediment collected by the passive sediment traps from being resuspended and washed out by river currents (Charlton 1983; Marvin et al. 2004). Suspended sediments collected by the trap tubes were retrieved and transferred into glass containers on-site and brought ashore for subsequent processing. Trap tubes were thoroughly washed and redeployed by positioning them back into the trap assemblages.

For the analysis of dissolved and particulate ⁷Be and ²¹⁰Pb, water samples (120 liters) from ~ 15 cm below the air–water interface were filtered through a pre-cleaned polypropylene filter cartridge (0.5- μ m median pore size) using a peristaltic pump and collected in six acid-cleaned 20-liter cubitainers (Trimble 2003). The used filter cartridge was utilized for the measurements of particulate ⁷Be and ²¹⁰Pb. One-liter water samples were collected (same depth as the 120-liter volume samples) in a pre-cleaned Nalgene bottle for suspended particulate matter (SPM) determination. SPM concentrations (mg L⁻¹) were determined gravimetrically by filtering 0.5 liters of river water through a preweighed 47-mm-diameter Nuclepore filter paper (0.4- μ m pore size) (Trimble and Baskaran 2005). We used 0.5- μ m (nominal)

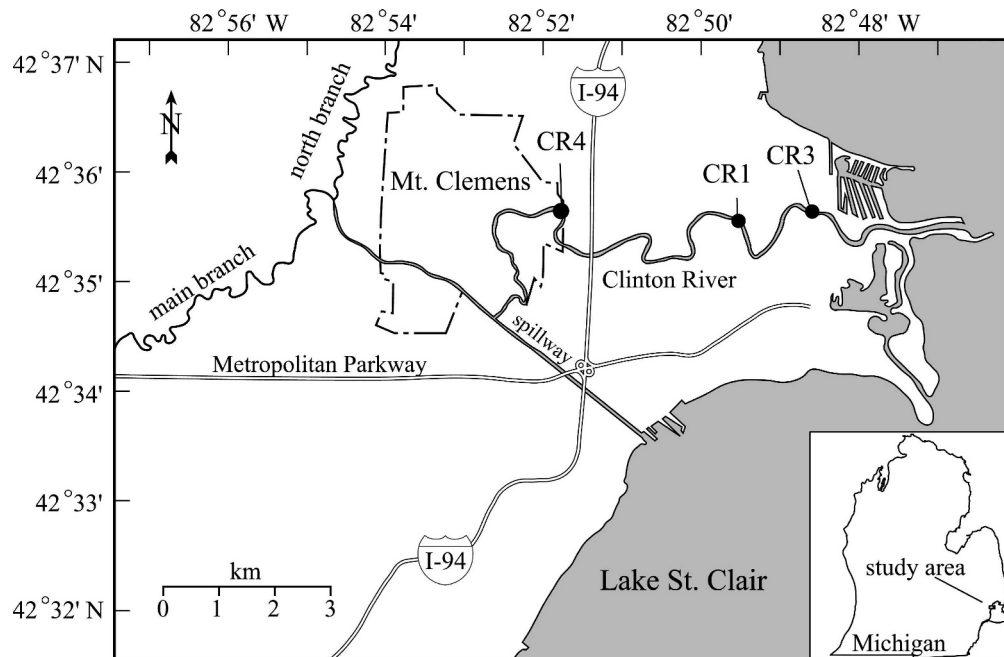


Fig. 1. Map of the main branch of the Clinton River, spillway, and western portion of Lake St. Clair, in southeast Michigan. Sediment trap locations CR1, CR3, and CR4 are represented by the closed circles.

Table 1. Locations of collecting stations, analyses performed at each station, and the corresponding samples. SPM, suspended particulate matter concentrations.

| Sta. | Latitude N | Longitude W | Analyses | Samples |
|------|-------------|-------------|---|--|
| CR1 | 42°35'47.1" | 82°49'33.4" | $^{210}\text{Pb}_{\text{xs}}$ and ^7Be in traps | CR1-1, CR1-2, CR1-3, CR1-4, CR1-5, CR1-6, CR1-7, CR1-8, CR1-9 |
| CR3 | 42°35'51.0" | 82°48'32.9" | SPM and ^{210}Pb and ^7Be in dissolved, particulate, bottom sediments, and sediment traps | CR3-2, CR3-3, CR3-4, CR3-5, CR3-6, CR3-7, CR3-8, CR3-9, CR3-10 |
| CR4 | 42°35'51.0" | 82°51'45.8" | SPM and ^{210}Pb and ^7Be in dissolved, particulate, bottom sediments, and sediment traps | CR4-2, CR4-3, CR4-4, CR4-5, CR4-6, CR4-7, CR4-8, CR4-9, CR4-10 |

cartridge-wound filters for the partitioning study of dissolved and particulate ^7Be and ^{210}Pb , and 0.4- μm (cut-off) filters for the measurements of SPM concentrations. It is not possible to filter 120 liters through 0.4- μm Nuclepore filter paper, and hence the concentration of dissolved ^7Be and ^{210}Pb is likely an overestimate, while the concentration of particulate ^7Be and ^{210}Pb is an underestimate compared to SPM filtration. However, we believe the difference between the concentration of radionuclides and SPM filtered through 0.4- μm and 0.5- μm filters is likely negligible. An Eckman dredge was used to retrieve the upper 2–3 cm of river-bottom sediments near the sediment traps.

Laboratory analysis—Sediment trap and bottom sediment samples were homogenized and dried at 50°C in a convection oven for 2–3 d. Dried samples (~10–15 g of bottom sediments and <1 to ~15 g of trap material) were pulverized and packed into gamma-counting vials for measurements of ^{210}Pb , ^{226}Ra , and ^7Be . The activities of ^7Be and ^{210}Pb were decay-corrected to the time of collection for bottom sediments, while the ^7Be activities for trapped sediments were decay-corrected to the mid-deployment period of the sediment trap.

$$\text{Decay-corrected } ^7\text{Be} = \text{uncorrected } ^7\text{Be} \times e^{\lambda_{\text{Be}}t_1} (1 - e^{-\lambda_{\text{Be}}t_2}) / (\lambda_{\text{Be}}t_2) \quad (1)$$

where λ_{Be} is the decay constant of ^7Be , t_1 is the time elapsed between end of collection and midcounting, and t_2 is the time elapsed between deployment and retrieval.

The used prefilter fiber was separated from the cartridge core, packed into a high-temperature-resistant crucible, and then ashed in a furnace at 550°C for ~4 h. The ash was quantitatively transferred from the crucible, weighed, and packed into a vial for gamma counting. Sediment mass fluxes collected in traps were determined gravimetrically. The elemental analysis (Al, Pb, and Be) of sediment trap material was completed by Actlabs in Ancaster, Ontario, using total digestion of dried sediment samples. The concentrations of Al, Pb, and Be were determined using an inductively coupled plasma-mass spectrometer (ICP-MS) that had detection limits of 0.01 wt%, 0.01 ppm, and 0.1 ppm, respectively.

Water samples brought back to the laboratory were transferred into a 200-liter low-density polyethylene drum.

The cubitainers were rinsed with 50 mL of concentrated HCl to remove any ^7Be and/or ^{210}Pb , and the rinse was added to the 200-liter container. To the solution, 1 mL of stable Be (= 1 mg), 1 mL of stable Pb (= 1 mg), ~20 g of NH_4Cl , and 12 mL of FeCl_3 (1 mL = 50 mg Fe) were added. The solution was stirred continuously for 10 min and then allowed to equilibrate overnight. After the solution had equilibrated, NH_3OH solution was added until pH reached 7 and $\text{Fe}(\text{OH})_3$ precipitated. $\text{Fe}(\text{OH})_3$ was allowed to settle for ~8 h. The precipitate and solution were separated by decanting followed by centrifugation. The precipitate was dissolved in 6 mol L^{-1} HCl, transferred to a 100-mL Teflon beaker, and dried completely. The residue was quantitatively transferred to a 10-mL vial with a minimal amount of 6 mol L^{-1} HCl.

The concentrations of ^{210}Pb , ^{226}Ra , and ^7Be in suspended particulate matter, bottom sediments, and trap materials (only ^7Be and ^{210}Pb in dissolved samples) were measured using a Canberra high-purity Ge-well detector coupled to a Canberra InSpector multichannel analyzer. The gamma-ray detector was calibrated with sediment standards obtained from the International Atomic Energy Agency (IAEA). Sediment standard RGU-1 for ^{210}Pb (46.5 keV) and ^{226}Ra (via ^{214}Pb and ^{214}Bi , 351.6 keV and 609.4 keV, respectively) was used. For ^7Be (477.6 keV), the counting efficiency was obtained from the linear extrapolation of the counting efficiencies obtained for ^{214}Pb and ^{214}Bi . The value was compared to the value obtained using traceable standards of ^7Be from the National Institute of Standards and Technology (NIST), and the values were in good agreement. Typical resolution (full-width at half-maximum) was about 1.3 keV at 46 keV and 2.2 keV at 1.33 MeV (Baskaran et al. 1996). The activities of ^7Be were decay-corrected to the date of sampling.

Results and discussion

Temperature, dissolved oxygen, salinity, and SPM—Temperature, salinity, and dissolved oxygen (DO) values are given in Table 2. These values are representative of the dates of collection rather than a continuous measurement in the river and do not include values in the winter, as no samples were collected when ice cover was present. River-water temperatures ranged from 6°C in mid-November

Table 2. Trap deployment interval, mass flux, water temperature, dissolved oxygen (DO), salinity, specific activities, and fluxes of ^7Be and $^{210}\text{Pb}_{\text{xs}}$ in the Clinton River, southeast Michigan. NM, not measured.

| Sample* | Trap deployment-trap retention | Days deployed | Temp. (°C) | DO (mg L ⁻¹) | Salinity | ^7Be (dpm g ⁻¹) | $^{210}\text{Pb}_{\text{xs}}$ (dpm g ⁻¹) | Mass flux (mg cm ⁻² d ⁻¹) [†] | ^7Be flux (dpm cm ⁻² d ⁻¹) | $^{210}\text{Pb}_{\text{xs}}$ flux (dpm cm ⁻² d ⁻¹) |
|---------|--------------------------------|---------------|------------|--------------------------|----------|--------------------------------------|--|---|--|--|
| CR1-1 | 02 Sep 04-02 Oct 04 | 30 | NM | NM | NM | 18.8±0.6 | 12.5±0.5 | 12.2 | 0.23±0.01 | 0.15±0.01 |
| CR1-2 | 24 Oct 04-31 Oct 04 | 7 | NM | NM | NM | 20.4±0.5 | 11.3±0.5 | 26.9 | 0.55±0.01 | 0.30±0.01 |
| CR3-2 | 24 Oct 04-31 Oct 04 | 7 | 14.10 | 0.17 | 0.3 | 18.9±1.0 | 11.6±0.9 | 6.6 | 0.12±0.01 | 0.08±0.01 |
| CR4-2 | 24 Oct 04-31 Oct 04 | 7 | NM | NM | NM | NM | NM | 34.7 | NM | NM |
| CR1-3 | 31 Oct 04-07 Nov 04 | 7 | NM | NM | NM | 30.9±0.8 | 14.1±0.7 | 48.5 | 1.50±0.04 | 0.68±0.03 |
| CR3-3 | 31 Oct 04-07 Nov 04 | 7 | 8.90 | 4.64 | 0.4 | 27.6±0.7 | 14.0±0.6 | 17.8 | 0.49±0.01 | 0.25±0.01 |
| CR4-3 | 31 Oct 04-07 Nov 04 | 7 | NM | NM | NM | 37.3±0.8 | 14.8±0.6 | 38.9 | 1.45±0.03 | 0.58±0.02 |
| CR1-4 | 07 Nov 04-14 Nov 04 | 7 | NM | NM | NM | 19.4±0.8 | 12.5±0.7 | 5.5 | 0.11±0.00 | 0.07±0.00 |
| CR3-4 | 07 Nov 04-14 Nov 04 | 7 | 6.40 | NM | 0.5 | 22.8±1.2 | 13.3±0.8 | 4.9 | 0.11±0.01 | 0.06±0.00 |
| CR4-4 | 07 Nov 04-14 Nov 04 | 7 | 6.30 | 3.03 | 0.5 | 21.0±1.1 | 12.1±0.7 | 4.2 | 0.09±0.00 | 0.05±0.00 |
| CR1-5 | 07 Nov 04-05 Dec 04 | 28 | NM | NM | NM | 29.8±0.8 | 13.3±0.5 | 29.8 | 0.89±0.02 | 0.40±0.02 |
| CR3-5 | 07 Nov 04-05 Dec 04 | 28 | NM | NM | NM | 24.7±0.8 | 12.4±0.6 | 17.9 | 0.44±0.01 | 0.22±0.01 |
| CR4-5 | 07 Nov 04-05 Dec 04 | 28 | NM | NM | NM | 25.3±0.8 | 15.2±0.6 | 22.9 | 0.58±0.02 | 0.35±0.01 |
| CR1-6 | 05 Dec 04-08 Apr 05 | 124 | NM | NM | NM | 20.6±0.6 | 12.7±0.4 | 30.2 | 0.62±0.02 | 0.38±0.01 |
| CR3-6 | 05 Dec 04-08 Apr 05 | 124 | 12.10 | 4.92 | 0.6 | 25.8±0.9 | 13.2±0.5 | 15.7 | 0.41±0.01 | 0.21±0.01 |
| CR4-6 | 05 Dec 04-08 Apr 05 | 124 | 12.70 | 7.29 | 0.6 | 21.0±0.9 | 13.1±0.5 | 26.7 | 0.56±0.02 | 0.35±0.01 |
| CR1-7 | 08 Apr 05-03 May 05 | 25 | NM | NM | NM | 13.3±0.6 | 9.34±0.6 | 28.1 | 0.37±0.02 | 0.26±0.02 |
| CR3-7 | 08 Apr 05-03 May 05 | 25 | 9.70 | 2.79 | 0.6 | 12.7±0.6 | 12.2±0.6 | 19.7 | 0.25±0.01 | 0.24±0.01 |
| CR4-7 | 08 Apr 05-03 May 05 | 25 | 9.90 | 5.33 | 0.6 | 16.4±0.7 | 10.4±0.6 | 22.5 | 0.37±0.01 | 0.23±0.01 |
| CR1-8 | 03 May 05-09 Jun 05 | 37 | NM | NM | NM | 10.9±0.7 | 9.97±0.5 | 25.8 | 0.28±0.02 | 0.26±0.01 |
| CR3-8 | 03 May 05-04 Jun 05 | 32 | 23.00 | 6.2 | 0.6 | 10.7±0.7 | 10.7±0.5 | 19.7 | 0.21±0.01 | 0.21±0.01 |
| CR4-8 | 03 May 05-04 Jun 05 | 32 | 21.00 | 3.58 | 0.7 | 20.5±0.9 | 11.7±0.6 | 23.4 | 0.48±0.02 | 0.27±0.01 |
| CR1-9 | 09 Jun 05-07 Jul 05 | 28 | NM | NM | NM | 22.2±1.2 | 14.3±0.6 | 10.0 | 0.22±0.01 | 0.14±0.01 |
| CR3-9 | 04 Jun 05-07 Jul 05 | 33 | 26.30 | 4.3 | 0.6 | 12.9±1.1 | 10.7±0.6 | 9.78 | 0.13±0.01 | 0.10±0.01 |
| CR4-9 | 04 Jun 05-07 Jul 05 | 33 | 21.60 | 3.1 | 0.5 | 30.2±1.3 | 14.3±0.5 | 20.8 | 0.63±0.03 | 0.30±0.01 |
| CR3-10 | 07 Jul 05-22 Aug 05 | 46 | NM | NM | NM | 14.6±0.9 | 12.3±0.5 | 29.6 | 0.43±0.03 | 0.36±0.02 |
| CR4-10 | 07 Jul 05-22 Aug 05 | 46 | NM | NM | NM | 27.7±1.2 | 12.1±0.6 | 73.2 | 2.03±0.09 | 0.89±0.04 |

*Only sediment trap samples were collected at sta. CR1.

†Surface area of the sediment trap = 70.8 cm².

Table 3. SPM concentration, and activities of ^7Be and ^{210}Pb in dissolved (A_i^d), particulate (A_i^p), specific (A_i^{SA}), trap (A_i^t), and bottom sediments (A_i^{bs}). NM, not measured; BD, below detection.

| Sample* | ^7Be | | | | | | | | | | ^{210}Pb | | | | | |
|---------|-----------------------|-----------------------|----------------------------|----------------------------|------------------------|------------------------|------------------------|----------------------------|----------------------------|------------------------|------------------------|------------------------|----------------------------|------------------------|------------------------|------------------------|
| | $A_{Be}^s : A_{Pb}^s$ | SPM | A_{Be}^d | A_{Be}^p | A_{Be}^{SA} | A_{Be}^s | A_{Be}^{bs} | A_{Pb}^d | A_{Pb}^p | A_{Pb}^{SA} | A_{Pb}^s | A_{Pb}^{bs} | A_{Pb}^t | A_{Pb}^{SA} | A_{Pb}^s | A_{Pb}^{bs} |
| | | (mg L ⁻¹) | (dpm 100 L ⁻¹) | (dpm 100 L ⁻¹) | (dpm g ⁻¹) | (dpm g ⁻¹) | (dpm g ⁻¹) | (dpm 100 L ⁻¹) | (dpm 100 L ⁻¹) | (dpm g ⁻¹) | (dpm g ⁻¹) | (dpm g ⁻¹) | (dpm 100 L ⁻¹) | (dpm g ⁻¹) | (dpm g ⁻¹) | (dpm g ⁻¹) |
| CR3-2 | 1.64±0.15 | 15.4 | 601±21 | 72.5±1.9 | 47.1±1.2 | 18.9±1.0 | 6.5±0.3 | 111±5 | 34.6±1.6 | 22.5±1.1 | 11.6±0.9 | 9.8±0.4 | 22.5±1.1 | 11.6±0.9 | 9.8±0.4 | 9.8±0.4 |
| CR4-2 | NM | 7.4 | 232±9 | 58.9±1.7 | 79.6±2.2 | NM | 6.3±0.3 | 47.9±3.3 | 25.3±1.2 | 34.2±1.7 | NM | 10.4±0.5 | 34.2±1.7 | NM | 10.4±0.5 | 10.4±0.5 |
| CR3-3 | 1.97±0.10 | 13.4 | 69.7±5.1 | 38.5±1.6 | 28.7±1.2 | 27.6±0.7 | 6.4±0.4 | 14.7±3.7 | 27.4±1.6 | 20.5±1.2 | 14.0±0.6 | 9.5±0.5 | 20.5±1.2 | 14.0±0.6 | 9.5±0.5 | 9.5±0.5 |
| CR4-3 | 2.52±0.11 | 3.4 | NM | 31.4±1.6 | 92.4±5 | 37.3±0.8 | 4.7±0.4 | NM | 16.7±1.4 | 49.0±4.2 | 14.8±0.6 | 6.8±0.4 | 49.0±4.2 | 14.8±0.6 | 6.8±0.4 | 6.8±0.4 |
| CR3-4 | 1.72±0.14 | 2.6 | NM | 10.4±1.3 | 40.0±4.9 | 22.8±1.2 | 11.6±0.5 | NM | 8.3±1.0 | 32.1±3.8 | 13.3±0.8 | 11.3±0.5 | 32.1±3.8 | 13.3±0.8 | 11.3±0.5 | 11.3±0.5 |
| CR4-4 | 1.74±0.13 | 2.2 | 36.2±3.0 | 18.5±2.5 | 84.1±11.0 | 21.0±1.1 | 2.6±0.4 | 10.1±2.1 | 14.4±2.4 | 65.6±11 | 12.1±0.7 | 4.0±0.4 | 65.6±11 | 12.1±0.7 | 4.0±0.4 | 4.0±0.4 |
| CR3-5 | 2.00±0.11 | 3.8 | 92.1±4.9 | 53.4±1.8 | 140±5.0 | 24.7±0.8 | BD | 18.8±3.2 | 30.8±1.6 | 81.1±4.3 | 12.4±0.6 | 4.3±0.4 | 81.1±4.3 | 12.4±0.6 | 4.3±0.4 | 4.3±0.4 |
| CR4-5 | 1.67±0.08 | 4.4 | 71.5±4.7 | 16.4±1.3 | 37.3±2.9 | 25.3±0.8 | 12.8±0.4 | 6.2±3.0 | 5.6±1.1 | 12.8±2.5 | 15.2±0.6 | 9.4±0.4 | 12.8±2.5 | 15.2±0.6 | 9.4±0.4 | 9.4±0.4 |
| CR3-6 | 1.96±0.11 | 17.6 | BD | 26.7±1.5 | 15.2±0.9 | 25.8±0.9 | 8.8±0.4 | BD | 28.7±1.7 | 16.3±1.0 | 13.2±0.5 | 12.3±0.5 | 16.3±1.0 | 13.2±0.5 | 12.3±0.5 | 12.3±0.5 |
| CR4-6 | 1.60±0.09 | 11.8 | 35.4±3.6 | 14.9±1.2 | 12.7±1.0 | 21.0±0.9 | BD | 8.9±2.0 | 11.5±1.2 | 9.7±1.1 | 13.1±0.5 | 3.2±0.4 | 9.7±1.1 | 13.1±0.5 | 3.2±0.4 | 3.2±0.4 |
| CR3-7 | 1.04±0.07 | 4.4 | 28.4±2.9 | 11.3±0.9 | 25.6±2.1 | 12.7±0.6 | 3.3±0.3 | 10.1±2.4 | 12.6±0.9 | 28.7±2.1 | 12.2±0.6 | 8.7±0.4 | 28.7±2.1 | 12.2±0.6 | 8.7±0.4 | 8.7±0.4 |
| CR4-7 | 1.58±0.11 | 7.0 | 29.7±3.6 | 7.5±0.9 | 10.7±1.3 | 16.4±0.7 | 6.3±0.3 | 12.6±2.4 | 3.2±0.9 | 4.6±1.3 | 10.4±0.6 | 6.0±0.4 | 4.6±1.3 | 10.4±0.6 | 6.0±0.4 | 6.0±0.4 |
| CR3-8 | 1.00±0.08 | 14.0 | 17.0±2.9 | 9.2±1.0 | 6.6±0.7 | 10.7±0.7 | BD | 11.7±2.6 | 13.7±1.1 | 9.8±0.8 | 10.7±0.5 | 8.4±0.4 | 9.8±0.8 | 10.7±0.5 | 8.4±0.4 | 8.4±0.4 |
| CR4-8 | 1.76±0.12 | 36.2 | 37.0±3.8 | 13.6±1.0 | 3.8±0.3 | 20.5±0.9 | 1.3±0.3 | 22.7±3.9 | 10.2±1.0 | 2.8±0.3 | 11.7±0.6 | 6.6±0.4 | 2.8±0.3 | 11.7±0.6 | 6.6±0.4 | 6.6±0.4 |
| CR3-9 | 1.21±0.12 | 6.2 | 113±6 | 21.6±0.8 | 34.9±1.4 | 12.9±1.1 | 2.0±0.5 | 25.9±2.9 | 10.1±0.7 | 16.3±1.2 | 10.7±0.6 | 8.9±0.4 | 16.3±1.2 | 10.7±0.6 | 8.9±0.4 | 8.9±0.4 |
| CR4-9 | 2.11±0.12 | 4.8 | 102±6 | 16.7±1.0 | 34.7±2.0 | 30.2±1.3 | 6.6±0.6 | 27.8±3.6 | 8.6±0.9 | 17.9±1.8 | 14.3±0.5 | 8.7±0.4 | 17.9±1.8 | 14.3±0.5 | 8.7±0.4 | 8.7±0.4 |
| CR3-10 | 1.19±0.09 | 21.2 | 55.0±4.3 | 17.9±1.1 | 8.5±0.5 | 14.6±0.9 | 5.4±0.3 | 20.3±2.5 | 14.3±1.1 | 6.8±0.5 | 12.3±0.5 | 11.2±0.4 | 6.8±0.5 | 12.3±0.5 | 11.2±0.4 | 11.2±0.4 |
| CR4-10 | 2.28±0.15 | 12.4 | 71.2±5.0 | 19.6±1.2 | 15.8±1.0 | 27.7±1.2 | BD | 43.0±4.0 | 9.22±1.1 | 7.4±0.9 | 12.1±0.6 | 5.0±0.4 | 7.4±0.9 | 12.1±0.6 | 5.0±0.4 | 5.0±0.4 |

* In two samples (CR3-2 and CR4-2), particulate and dissolved ^7Be and ^{210}Pb activities were anomalously high.

2004 to 26°C in early July 2005 and generally fluctuated with seasonal changes. Salinities varied from 0.3‰ to 0.7‰ (approximately two orders of magnitude lower than seawater), and dissolved oxygen values varied from 0.17 to 7.29 mg L⁻¹. Suspended particulate matter (SPM) concentrations (mg L⁻¹), shown in Table 3, in the Clinton River varied from 2.2 to 36.2 mg L⁻¹ (GM, geometric mean: 7.8 mg L⁻¹) in November 2004 and June 2005, respectively. SPM concentrations varied as a function of river discharge and were typically higher in the spring and fall months and lower in the winter and summer months.

Activities of dissolved and particulate ^7Be and ^{210}Pb —The activities of ^{210}Pb and ^7Be in the dissolved (A_{Pb}^d and A_{Be}^d) and particulate (A_{Pb}^p and A_{Be}^p) phases, trapped sediments, and bottom sediments are given in Table 3. We report the averages of radionuclide activities in the water column and sediments (all stations). Averages reported in this study were weighted and calculated as geometric means (GM) to minimize the influence of unusually high or low values. The specific activities (= dpm g⁻¹ of particulate matter) of ^7Be and ^{210}Pb varied from 3.8 to 140 dpm g⁻¹ (GM: 26.3 dpm g⁻¹, $n = 18$) and from 2.8 to 81.1 dpm g⁻¹ (GM: 17.0 dpm g⁻¹, $n = 18$), respectively. The process most likely responsible for such large variations in dissolved and particulate ^7Be and ^{210}Pb activities is particle resuspension associated with rainstorms, spring melting, and high seasonal river flows. The higher dissolved and particulate ^7Be activities are partly attributed to higher atmospheric depositional fluxes of ^7Be compared to ^{210}Pb . For example, up to a factor of ~20 difference in the atmospheric depositional fluxes of ^7Be and ^{210}Pb (3.1–63 dpm cm⁻² yr⁻¹ for ^7Be and 0.35–10.3 cm⁻² yr⁻¹ for ^{210}Pb) in Detroit, Michigan, was reported by McNeary and Baskaran (2003), where the highest depositional fluxes corresponded to the highest amounts of precipitation.

The particulate fractions (f_i = particulate activity/total activity) of ^7Be or ^{210}Pb , which ranged from 11% to 37% for ^7Be (GM: 23% ± 8%, $n = 15$) and from 18% to 65% for ^{210}Pb (GM: 38% ± 17%, $n = 15$), were significantly lower than the values reported in other freshwater systems (such as ~85% in the coastal waters of Lake Superior [Chai and Urban 2004] and ~76% in Lake Sammamish, Washington [Balistreri et al. 1995]). Although the riverine system is much more dynamic than coastal lake waters, the relatively lower values of f_i for both ^7Be and ^{210}Pb (<50%) in the riverine system are intriguing. We hypothesize that this is due to the presence of submicronic particulate matter (colloidal). Visual observations showed that the water was murky after filtration through the 0.5- μm filter cartridge, supporting this hypothesis. There is no correlation ($R = 0.1$, not shown) between SPM concentration and f_i , even though we expect f_i to increase with higher SPM concentrations. This is likely due to a greater degree of complexation of ^7Be and ^{210}Pb with colloids (<0.5 μm) than with particulate matter (>0.5 μm) in the water column.

Sediment traps—Mass fluxes and specific activities of ^7Be and $^{210}\text{Pb}_{\text{xs}}$: The duration of deployment of sediment

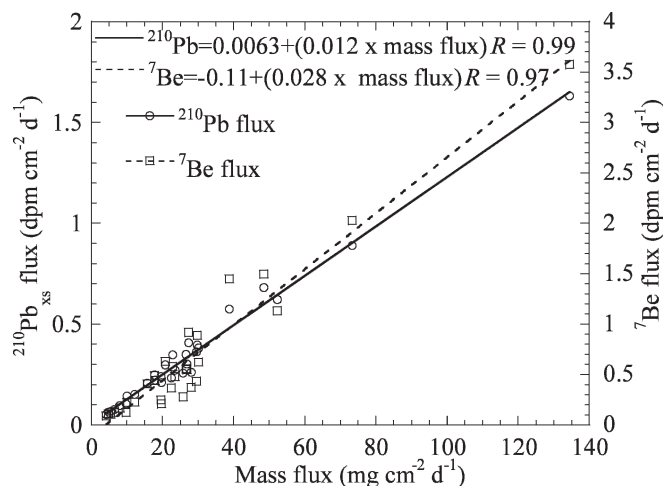


Fig. 2. Mass fluxes vs. ${}^7\text{Be}$ and ${}^{210}\text{Pb}_{\text{xs}}$ fluxes.

traps, mass flux, fluxes of ${}^7\text{Be}$ and ${}^{210}\text{Pb}_{\text{xs}}$ (${}^{210}\text{Pb}$ in excess of parent supported ${}^{210}\text{Pb}$), and specific activities are given in Table 2. The mass fluxes varied considerably from $4.2 \text{ mg cm}^{-2} \text{ d}^{-1}$ to $134 \text{ mg cm}^{-2} \text{ d}^{-1}$ (GM: $20.5 \text{ mg cm}^{-2} \text{ d}^{-1}$), and the highest values occurred in late summer and early autumn (data not shown); this was attributable to increased erosional input and resuspension of bottom sediments following heavy rainstorms and spring melting. Although there is no direct way to quantify the under/overtrapping of this sediment trap (as with ${}^{234}\text{Th}$ in shallow waters or ${}^{230}\text{Th}$ in deep waters in marine environments), the mass fluxes obtained from two trap tubes deployed at any given site agreed within $\sim 10\%$.

Due to ${}^{222}\text{Rn}$ loss from particle surfaces, a correction for the parent-supported ${}^{210}\text{Pb}$ needed to be applied. Based on a large number of experiments on suspended particulate matter, Imboden and Stiller (1982) recommended using a value 50% of ${}^{226}\text{Rn}$, which we used in this work. Such a correction resulted in subtraction of a value of $\sim 10\%$ (with ${}^{210}\text{Pb}_{\text{parent-supported}}/{}^{210}\text{Pb}_{\text{total}}$ ratio = $\sim 20\%$) from the total ${}^{210}\text{Pb}$ activity. The ${}^7\text{Be}$ and ${}^{210}\text{Pb}_{\text{xs}}$ fluxes varied from 0.11 to $3.58 \text{ dpm cm}^{-2} \text{ d}^{-1}$ (GM: $0.42 \text{ dpm cm}^{-2} \text{ d}^{-1}$, $n = 30$) and from 0.05 to $1.63 \text{ dpm cm}^{-2} \text{ d}^{-1}$ (GM: $0.25 \text{ dpm cm}^{-2} \text{ d}^{-1}$, $n = 30$), respectively, and showed a strong correlation with mass fluxes (for ${}^7\text{Be}$, $R = 0.97$, $p < 0.001$; for ${}^{210}\text{Pb}$, $R = 0.99$, $p < 0.001$) (Fig. 2). There was also a strong correlation between mass fluxes and Al fluxes (data not shown, $R = 0.91$, $p < 0.001$), suggesting that the settling material was composed mainly of terrigenous materials. Strong correlations between mass fluxes and fluxes of stable Be (Fig. 3; $R = 0.97$, $p < 0.001$) and Pb (Fig. 3; $R = 0.95$, $p < 0.001$) were also observed, suggesting that ${}^7\text{Be}$ and ${}^{210}\text{Pb}$ can be used as tracers of stable Be and Pb, respectively, in the riverine system.

The calculated annual fluxes of ${}^7\text{Be}$ and ${}^{210}\text{Pb}_{\text{xs}}$ ranged from 127 to $291 \text{ dpm cm}^{-2} \text{ yr}^{-1}$ (GM: $188 \text{ dpm cm}^{-2} \text{ yr}^{-1}$) and from 82 to $152 \text{ dpm cm}^{-2} \text{ yr}^{-1}$ (GM: $110 \text{ dpm cm}^{-2} \text{ yr}^{-1}$), respectively. Note that the trap sediments were deployed but were not collected in between early December and early April, but they were collected in mid-April, and hence our flux values are accurate for ${}^{210}\text{Pb}$ because of its long half-life. Since the mid-deployment time is

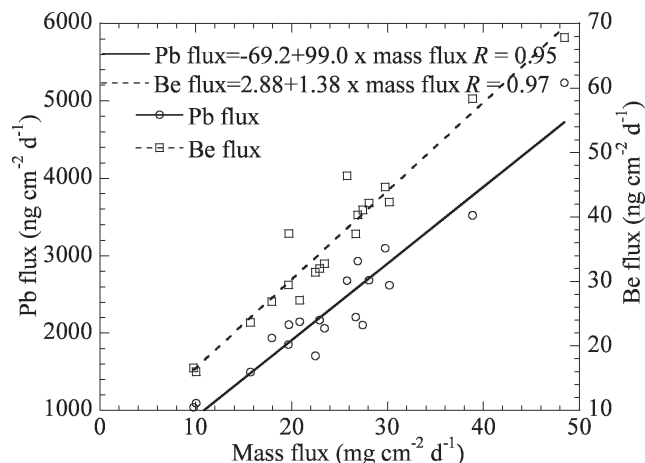


Fig. 3. Mass fluxes vs. Be and Pb fluxes.

comparable to the mean life of ${}^7\text{Be}$, and ${}^7\text{Be}$ activities were decay-corrected from the midcollection to midcounting period and for the decay during the deployment period, the ${}^7\text{Be}$ flux values are also expected to be accurate.

Direct atmospheric deposition accounts for only $\sim 7\%$ of the ${}^7\text{Be}$ and only $\sim 2\%$ of the ${}^{210}\text{Pb}_{\text{xs}}$ in the sediment traps, indicating that most of the ${}^7\text{Be}$ and ${}^{210}\text{Pb}_{\text{xs}}$ fluxes were delivered by additional sources. Particle resuspension is likely the primary source of elevated ${}^7\text{Be}$ and ${}^{210}\text{Pb}_{\text{xs}}$ activities in the sediment traps, which is expected in a turbulent river system. Although no previous data exist for riverine systems, similar findings have been reported in the shallow turbulent Øresund Sound (only $\sim 5\%$ of ${}^{210}\text{Pb}$ fluxes were derived from atmospheric deposition), which connects the Baltic and North Seas (Roos and Valeur 2006).

${}^7\text{Be} : {}^{210}\text{Pb}_{\text{xs}}$ activity ratios as indicators of resuspension—
The ${}^7\text{Be} : {}^{210}\text{Pb}_{\text{xs}}$ activity ratios in sediment trap material (Table 3) ranged from 1.00 to 2.52 (GM: 1.69 ± 0.41 , $n = 30$). The ${}^7\text{Be} : {}^{210}\text{Pb}_{\text{xs}}$ activity ratios in trap material were less than those in the atmospheric deposition (average = 8.3) reported by McNeary and Baskaran (2003) for this region, indicating that there were additional sources of ${}^{210}\text{Pb}_{\text{xs}}$ in the trap material. However, the ${}^7\text{Be} : {}^{210}\text{Pb}_{\text{xs}}$ activity ratio in trap material was greater than the expected ratios of the sediment inventories of ${}^7\text{Be}$ and ${}^{210}\text{Pb}$ (${}^7\text{Be} : {}^{210}\text{Pb}_{\text{xs}}$), which is 0.055 (assuming 2.74 dpm cm^{-2} , based on the long-term annual fallout of $13 \text{ dpm cm}^{-2} \text{ yr}^{-1}$ for ${}^7\text{Be}$; 50.2 dpm cm^{-2} , based on the long-term annual fallout of $1.56 \text{ dpm cm}^{-2} \text{ yr}^{-1}$ for ${}^{210}\text{Pb}$; McNeary and Baskaran 2003). Resuspension of bottom sediments is a likely culprit of the additional ${}^{210}\text{Pb}_{\text{xs}}$ because of the remobilization of comparatively more sediment-bound ${}^{210}\text{Pb}_{\text{xs}}$ than ${}^7\text{Be}$ (due to the differences in their mean-lives). During frequent particle resuspension events, which result in high mass fluxes dominated by resuspended sediments, we expect to find lower ${}^7\text{Be} : {}^{210}\text{Pb}_{\text{xs}}$ activity ratios in trap material (e.g., Feng et al. 1999). However, we find that as mass flux increases, the ${}^7\text{Be} : {}^{210}\text{Pb}_{\text{xs}}$ activity ratio in trap material also slightly increases (Fig. 4; $R = 0.41$, $p < 0.05$), indicating that dissolved ${}^7\text{Be}$ may be preferentially scavenged by resuspended particles in the water column. A plot of ${}^{210}\text{Pb}_{\text{xs}}$ vs.

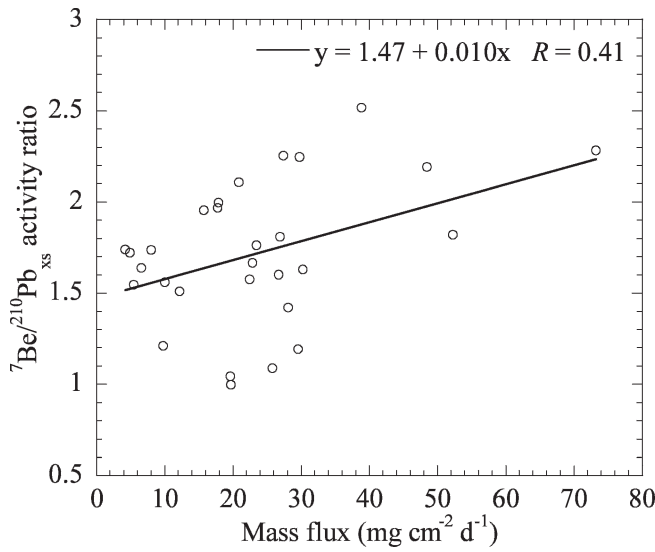


Fig. 4. Mass fluxes vs. ${}^7\text{Be}:$ ${}^{210}\text{Pb}_{\text{xs}}$ activity ratios in trapped sediments.

${}^7\text{Be}$ (Fig. 5) showing SPM, material collected in the trap, and bottom sediments indicates the following: (1) the ${}^7\text{Be}:$ ${}^{210}\text{Pb}_{\text{xs}}$ activity ratio in the trap sediments is the same as that in SPM, but is more than that in bottom sediments; (2) generally, the specific activity of ${}^7\text{Be}$ and ${}^{210}\text{Pb}$ in SPM is more than that in the trap sediments, which is more than that in bottom sediments; and (3) the linear correlation between ${}^7\text{Be}$ and ${}^{210}\text{Pb}$ is strong in SPM ($R = 0.94$), followed by the trap sediments ($R = 0.79$), and weakest with bottom sediments ($R = 0.56$). This pattern suggests that a major portion of the ${}^7\text{Be}$ and ${}^{210}\text{Pb}$ in SPM is derived from water-column scavenging compared to the trap sediments. The differences in the pattern can also be due to the differences between the median grain sizes of SPM (which is expected to be smaller compared to sediments in the trap) and trap material, although we do not have the grain-size data.

Modeling particulate ${}^7\text{Be}$ and ${}^{210}\text{Pb}_{\text{xs}}$ to quantify sediment resuspension rates—The rate of resuspension can be determined from a mass balance of particulate ${}^7\text{Be}$ and ${}^{210}\text{Pb}_{\text{xs}}$ (Fig. 6), which can be written as follows:

$$\Psi_{\text{Be}}^d A_{\text{Be}}^d + I_{\text{Be}}^{\text{rp}} + \frac{R_{\text{Be}} A_{\text{Be}}^r}{H} = O_{\text{Be}}^{\text{rp}} + \lambda_{\text{Be}} A_{\text{Be}}^p + \frac{R_{\text{Be}} A_{\text{Be}}^s}{H} \quad (2)$$

and

$$\Psi_{\text{Pb}}^d A_{\text{Pb}}^d + \lambda_{\text{Pb}} A_{\text{Pb}}^p + I_{\text{Pb}}^{\text{rp}} + \frac{R_{\text{Pb}} A_{\text{Pb}}^r}{H} = O_{\text{Pb}}^{\text{rp}} + \lambda_{\text{Pb}} A_{\text{Pb}}^p + \frac{R_{\text{Pb}} A_{\text{Pb}}^s}{H} \quad (3)$$

where $I_{\text{Be}}^{\text{rp}}$ and $I_{\text{Pb}}^{\text{rp}}$ are the riverine input flux of particulate ${}^7\text{Be}$ and ${}^{210}\text{Pb}_{\text{xs}}$ ($\text{dpm cm}^{-3} \text{ yr}^{-1}$), respectively, $O_{\text{Be}}^{\text{rp}}$ and $O_{\text{Pb}}^{\text{rp}}$ are the riverine output flux of particulate ${}^7\text{Be}$ and ${}^{210}\text{Pb}_{\text{xs}}$ ($\text{dpm cm}^{-3} \text{ yr}^{-1}$), respectively, H is the mean depth (200 cm), A_{Rn}^p is the activity of ${}^{222}\text{Rn}$ (dpm cm^{-3}) adsorbed onto particulate matter, A_{Be}^d and A_{Pb}^d are the

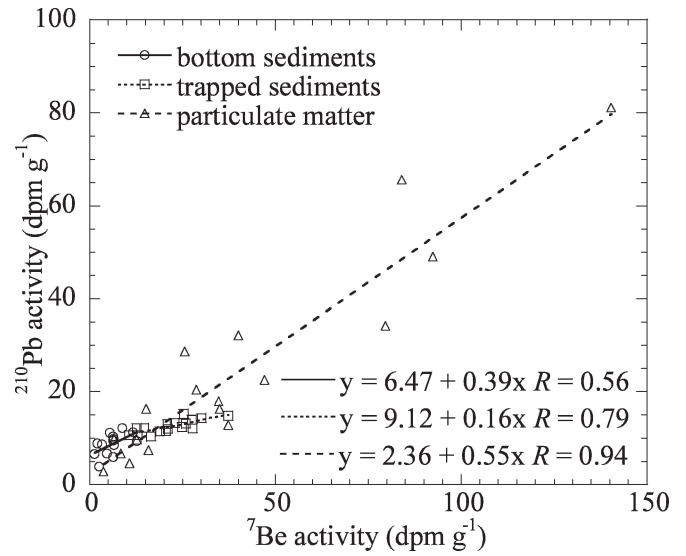


Fig. 5. ${}^7\text{Be}$ activities vs. ${}^{210}\text{Pb}_{\text{xs}}$ activities in bottom sediments, trapped sediments, and suspended particulate matter.

activities of dissolved ${}^7\text{Be}$ and ${}^{210}\text{Pb}$ (dpm cm^{-3}), A_{Be}^p and A_{Pb}^p are the activities of particulate ${}^7\text{Be}$ and ${}^{210}\text{Pb}_{\text{xs}}$ (dpm cm^{-3}), A_{Be}^r and A_{Pb}^r are the activities of ${}^7\text{Be}$ and ${}^{210}\text{Pb}_{\text{xs}}$ in the resuspended material (dpm g^{-1}), A_{Be}^s and A_{Pb}^s are the activities of ${}^7\text{Be}$ and ${}^{210}\text{Pb}_{\text{xs}}$ in the settling particulate matter collected in sediment traps (dpm g^{-1}), Ψ_{Be}^d and Ψ_{Pb}^d are the first-order removal rate constants of ${}^7\text{Be}$ and ${}^{210}\text{Pb}$ (yr^{-1}), and R_{Be} and R_{Pb} are sediment resuspension rates ($\text{g cm}^{-2} \text{ yr}^{-1}$) using ${}^7\text{Be}$ and ${}^{210}\text{Pb}_{\text{xs}}$, respectively.

For the resuspended material, we took the activities of the nuclides in the upper 1 cm of the bottom sediments, because this upper layer is likely the most frequently resuspended. The importance of the $\lambda_{\text{Pb}} A_{\text{Rn}}^p$ term can be evaluated as follows: Using the average particulate ${}^{226}\text{Ra}$ concentration of $2.0 \text{ dpm } 100 \text{ L}^{-1}$ (data not shown), then the calculated value of the term $\lambda_{\text{Pb}} A_{\text{Rn}}^p$ is $1.7 \times 10^{-9} \text{ dpm cm}^{-3} \text{ d}^{-1}$; taking the average concentration of dissolved ${}^{210}\text{Pb}$ to be $26.1 \text{ dpm } 100 \text{ L}^{-1}$ and an average value of Ψ_{Pb}^d of 0.14 d^{-1} , then the calculated value of the term $\Psi_{\text{Pb}}^d A_{\text{Pb}}^d$ is $3.6 \times 10^{-5} \text{ dpm cm}^{-3} \text{ d}^{-1}$, which is about 3–4 orders of magnitude higher than the production term from ${}^{222}\text{Rn}$ on the particulate matter; hence the radon production term is neglected in all calculations.

Assuming that ${}^7\text{Be}$ and ${}^{210}\text{Pb}_{\text{xs}}$ activities of the upper layer of bottom sediment are equal to those of resuspended sediment, $A_{\text{Be}}^r = A_{\text{Be}}^{\text{bs}}$ and $A_{\text{Pb}}^r = A_{\text{Pb}}^{\text{bs}}$, then the mass-balance equations for particulate ${}^7\text{Be}$ and ${}^{210}\text{Pb}_{\text{xs}}$ yield sediment resuspension rates ($\text{g cm}^{-2} \text{ yr}^{-1}$) using ${}^7\text{Be}$ and ${}^{210}\text{Pb}_{\text{xs}}$, respectively:

$$R_{\text{Be}} = H \times \frac{\Psi_{\text{Be}}^c A_{\text{Be}}^d - \lambda_{\text{Be}} A_{\text{Be}}^p}{A_{\text{Be}}^s - A_{\text{Be}}^r} \quad (4)$$

and

$$R_{\text{Pb}} = H \times \frac{\Psi_{\text{Pb}}^c A_{\text{Pb}}^d - \lambda_{\text{Pb}} A_{\text{Pb}}^p}{A_{\text{Pb}}^s - A_{\text{Pb}}^r} \quad (5)$$

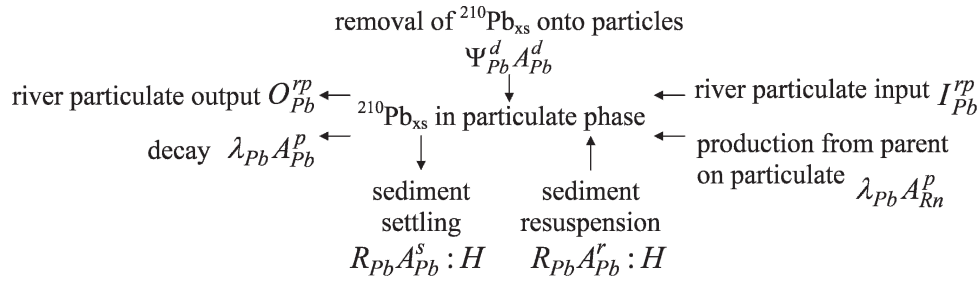


Fig. 6. Model showing all the sources and sinks of particulate ^{210}Pb in the Clinton River.

The resuspension rates calculated using ^7Be and $^{210}\text{Pb}_{\text{xs}}$ activities varied between 0.50 and $1.34 \text{ g cm}^{-2} \text{ yr}^{-1}$ (GM: $0.83 \pm 0.34 \text{ g cm}^{-2} \text{ yr}^{-1}$, $n = 10$) and between 0.16 and $1.49 \text{ g cm}^{-2} \text{ yr}^{-1}$ (GM: $0.38 \pm 0.38 \text{ g cm}^{-2} \text{ yr}^{-1}$, $n = 14$), respectively. Although there are no previously reported resuspension rates for riverine systems, we compared our values to those of Chai and Urban (2004), who calculated similar but slightly lower resuspension rates ($\sim 0.1 \text{ g cm}^{-2} \text{ yr}^{-1}$) using ^{210}Pb for the nearshore region of Lake Superior. Due to dynamic conditions, higher resuspension rates are expected in the river.

The annual mass fluxes determined from the total mass of trapped sediments, which ranged from 6.6 to $11.9 \text{ g cm}^{-2} \text{ yr}^{-1}$ (GM: $8.9 \text{ g cm}^{-2} \text{ yr}^{-1}$, $n = 3$), can be compared to the long-term ($\sim 100 \text{ yr}$) net sediment accumulation rates (SAR) obtained using $^{210}\text{Pb}_{\text{xs}}$ (GM: $0.88 \pm 0.38 \text{ g cm}^{-2} \text{ yr}^{-1}$, $n = 5$) at sites near the sediment traps. The relatively large discrepancy between the annual mass fluxes and the long-term net SAR is similar to discrepancies between mass fluxes and accumulation rates reported for the nearshore environment along Lake Superior (Urban et al. 2004). Highly elevated mass fluxes in sediment traps compared to SAR in the Niagara River near Lake Ontario were also observed by Charlton (1983), who hypothesized that sediments may be resuspended several times before being permanently deposited. Since resuspension rates only represent $\sim 10\text{--}20\%$ of the total mass flux, but direct atmospheric deposition accounts for $< 7\%$ of the ^7Be and $^{210}\text{Pb}_{\text{xs}}$ in the sediment traps, the discrepancy between mass fluxes and long-term net accumulation rates may provide insight into particle-recycling events in the river system, such that the number of multiple resuspension events for individual particles may be quantified. During such multiple resuspension events, the particulate matter can scavenge additional particle-reactive species from the water column. Furthermore, the desorption of particle-laden contaminants during multiple resuspension events could result in the mobility of contaminants to farther distances from the contaminated site.

Residence times and removal rates of dissolved ^7Be and ^{210}Pb —The residence times and removal rates of dissolved ^7Be and ^{210}Pb in the Clinton River (Table 4) can be calculated based on a simple box model, similar to the one used in other coastal and marine systems (Santschi et al. 1979; Baskaran et al. 1997; Baskaran and Santschi 2002). The model requires that all the inputs and outputs be accurately characterized. Although a riverine system is

much more dynamic than coastal, marine, or lacustrine systems, one can assume steady-state conditions under the assumption that advective inflow of water into the box equals advective outflow out of the box. The major inputs of dissolved ^{210}Pb into the box are: (1) Production from its grandparent ^{222}Rn (for ^{210}Pb); (2) atmospheric depositional input (^7Be and ^{210}Pb) at the air–water interface; and (3) river input of dissolved ^7Be and ^{210}Pb . The major outputs from this box are: (1) Decay of ^7Be and ^{210}Pb ; (2) removal of ^7Be and ^{210}Pb by scavenging onto particles; and (3) river output of dissolved ^7Be and ^{210}Pb . Furthermore, assuming that diffusive transport is negligible, the input of ^7Be and ^{210}Pb from desorption from particulate material is insignificant, and the in situ production of ^{210}Pb from ^{222}Rn is negligible (discussed earlier), then the mass-balance equations for dissolved ^7Be and ^{210}Pb can be written as:

$$I_{\text{Be}}^{\text{rd}} + I_{\text{Be}}^{\text{a}} = \lambda_{\text{Be}} A_{\text{Be}}^{\text{d}} + \Psi_{\text{Be}}^{\text{d}} A_{\text{Be}}^{\text{d}} + O_{\text{Be}}^{\text{rd}} \quad (6)$$

and

$$\lambda_{\text{Pb}} A_{\text{Rn}} + I_{\text{Pb}}^{\text{rd}} + I_{\text{Pb}}^{\text{a}} = \lambda_{\text{Pb}} A_{\text{Pb}}^{\text{d}} + \Psi_{\text{Pb}}^{\text{d}} A_{\text{Pb}}^{\text{d}} + O_{\text{Pb}}^{\text{rd}} \quad (7)$$

where λ_{Be} and λ_{Pb} are the decay constants of ^7Be ($= 4.75 \text{ yr}^{-1}$) and ^{210}Pb ($= 0.0311 \text{ yr}^{-1}$), respectively, $I_{\text{Be}}^{\text{rd}}$ and $I_{\text{Pb}}^{\text{rd}}$ are the riverine input fluxes of dissolved ^7Be and ^{210}Pb ($\text{dpm cm}^{-2} \text{ yr}^{-1}$), respectively, $O_{\text{Be}}^{\text{rd}}$ and $O_{\text{Pb}}^{\text{rd}}$ are the riverine output fluxes of dissolved ^7Be and ^{210}Pb ($\text{dpm cm}^{-2} \text{ yr}^{-1}$), respectively, I_{Be}^{a} and I_{Pb}^{a} are the atmospheric depositional fluxes of ^7Be ($= 13 \text{ dpm cm}^{-2} \text{ yr}^{-1}$) and ^{210}Pb ($= 1.56 \text{ dpm cm}^{-2} \text{ yr}^{-1}$), respectively, A_{Rn} is the inventory of ^{222}Rn (dpm cm^{-2}), and A_{Be}^{d} and A_{Pb}^{d} are the inventories of dissolved ^7Be and ^{210}Pb activities (dpm cm^{-2}).

The residence times of dissolved ^7Be ($\tau_{\text{Be}}^{\text{d}}$) and ^{210}Pb ($\tau_{\text{Pb}}^{\text{d}}$) can be calculated by rearranging Eqs. 6 and 7:

$$\tau_{\text{Be}}^{\text{d}} = \frac{1}{\Psi_{\text{Be}}^{\text{d}}} = \frac{A_{\text{Be}}^{\text{d}}}{-\lambda_{\text{Be}} A_{\text{Be}}^{\text{d}} + I_{\text{Be}}^{\text{rd}} + I_{\text{Be}}^{\text{a}} - O_{\text{Be}}^{\text{rd}}} \times 365 \quad (8)$$

and

$$\tau_{\text{Pb}}^{\text{d}} = \frac{1}{\Psi_{\text{Pb}}^{\text{d}}} = \frac{A_{\text{Pb}}^{\text{d}}}{\lambda_{\text{Pb}} (A_{\text{Rn}} - A_{\text{Pb}}^{\text{d}}) + I_{\text{Pb}}^{\text{rd}} + I_{\text{Pb}}^{\text{a}} - O_{\text{Pb}}^{\text{rd}}} \times 365 \quad (9)$$

where $\tau_{\text{Be}}^{\text{d}}$ and $\tau_{\text{Pb}}^{\text{d}}$ are the dissolved residence times of ^7Be and ^{210}Pb (d). Residence times of dissolved ^7Be and ^{210}Pb varied between 1 and 60 d (GM: $4.1 \pm 2.7 \text{ d}$, $n = 15$) and between 2.9 and 52 d (GM: $9.0 \pm 2.1 \text{ d}$, $n = 15$), respectively. Dissolved residence times were compared to

Table 4. Dissolved (τ_i^d) and particulate (τ_i^p) residence times, removal rates (Ψ_i^d), and resuspension rates (R_i) using ^7Be and $^{210}\text{Pb}_{\text{xs}}$. NM, not measured.

| Sample | ^7Be | | | | ^{210}Pb | | | | | |
|--------|---|-----------------------------|---|-----------------------------|---|---|-----------------------------|---|-----------------------------|---|
| | K_d^{Be} ($\times 10^5 \text{ cm}^3 \text{ g}^{-1}$)* | τ_{Be}^d (d) | Ψ_{Be}^d (d^{-1}) | τ_{Be}^p (d) | R_{Be} ($\text{g cm}^{-2} \text{ yr}^{-1}$) | K_d^{Pb} ($\times 10^5 \text{ cm}^3 \text{ g}^{-1}$)* | τ_{Pb}^d (d) | Ψ_{Pb}^d (d^{-1}) | τ_{Pb}^p (d) | R_{Pb} ($\text{g cm}^{-2} \text{ yr}^{-1}$) |
| CR3-2 | 0.078±0.003 | 60.3±2.1 | 0.02±0.001 | 2.1 | 0.53 | 0.20±0.01 (0.10±0.01) | 52±2.5 | 0.02±0.001 | 1.3 | 0.89 |
| CR4-2 | 0.34±0.02 (NM) | 15.7±0.6 | 0.06±0.002 | NM | NM | 0.71±0.06 (NM) | 22.5±1.5 | 0.05±0.003 | NM | NM |
| CR3-3 | 0.41±0.03 (0.40±0.03) | 4.1±0.3 | 0.24±0.018 | 1.7 | 0.57 | 1.4±0.4 (0.95±0.24) | 6.9±1.7 | 0.15±0.037 | 2.8 | 0.35 |
| CR4-3 | NM (NM) | NM | NM | NM | NM | NM (NM) | NM | NM | NM | NM |
| CR3-4 | NM (NM) | NM | NM | NM | NM | NM (NM) | NM | NM | NM | NM |
| CR4-4 | 2.3±0.4 (0.58±0.06) | 2.1±0.2 | 0.48±0.039 | 0.2 | 0.68 | 6.5±1.7 (1.20±0.26) | 4.7±1.0 | 0.21±0.044 | 0.8 | 0.19 |
| CR3-5 | 1.5±0.1 (0.27±0.02) | 5.6±0.3 | 0.18±0.010 | NM | NM | 4.3±0.8 (0.66±0.12) | 8.8±1.5 | 0.11±0.020 | 1.4 | 0.19 |
| CR4-5 | 0.52±0.05 (0.35±0.03) | 4.2±0.3 | 0.24±0.016 | 0.3 | 0.97 | 2.1±1.1 (2.44±1.19) | 2.9±1.4 | 0.34±0.167 | 1.2 | 0.27 |
| CR3-6 | NM (NM) | NM | NM | NM | NM | NM (NM) | NM | NM | NM | NM |
| CR4-6 | 0.36±0.05 (0.59±0.06) | 2.0±0.2 | 0.49±0.050 | NM | NM | 1.1±0.3 (1.47±0.34) | 4.2±1.0 | 0.24±0.055 | 5.5 | 0.16 |
| CR3-7 | 0.90±0.12 (0.45±0.05) | 1.6±0.2 | 0.61±0.062 | 0.2 | 1.34 | 2.8±0.7 (1.20±0.29) | 4.7±1.1 | 0.21±0.049 | 0.7 | 0.45 |
| CR4-7 | 0.36±0.06 (0.55±0.07) | 1.7±0.2 | 0.59±0.072 | 0.4 | 1.25 | 0.37±0.12 (0.83±0.16) | 5.9±1.1 | 0.17±0.032 | 1.5 | 0.35 |
| CR3-8 | 0.39±0.08 (0.63±0.11) | 1.0±0.2 | 1.04±0.175 | NM | NM | 0.84±0.19 (0.91±0.20) | 5.5±1.2 | 0.18±0.040 | 1.5 | 0.68 |
| CR4-8 | 0.10±0.01 (0.56±0.06) | 2.1±0.2 | 0.47±0.048 | 4.1 | 0.65 | 0.12±0.02 (0.51±0.09) | 10.7±1.8 | 0.09±0.016 | 8.6 | 0.31 |
| CR3-9 | 0.31±0.02 (0.11±0.01) | 6.9±0.4 | 0.14±0.007 | 0.4 | 1.07 | 0.63±0.08 (0.41±0.05) | 12.1±1.4 | 0.08±0.009 | 0.5 | 0.86 |
| CR4-9 | 0.34±0.03 (0.29±0.02) | 6.2±0.4 | 0.16±0.010 | 0.7 | 0.50 | 0.64±0.11 (0.51±0.07) | 13.1±1.7 | 0.08±0.010 | 1.3 | 0.27 |
| CR3-10 | 0.15±0.02 (0.27±0.03) | 3.2±0.3 | 0.31±0.024 | 1.2 | 1.33 | 0.33±0.05 (0.60±0.08) | 9.5±1.2 | 0.11±0.013 | 1.0 | 1.49 |
| CR4-10 | 0.22±0.02 (0.39±0.03) | 4.2±0.3 | 0.24±0.017 | NM | NM | 0.17±0.03 (0.28±0.03) | 20.2±1.9 | 0.05±0.005 | 4.2 | 0.22 |

* The K_d values of ^{210}Pb and ^7Be , using the relationship (A_i^p / A_i^d), are in parentheses.

lacustrine systems because there are no previously reported data for rivers. The values of τ_{Pb}^d fell within the range reported for other freshwater systems such as lakes: 1–40 d (Benoit and Hemond 1987; Balistreri et al. 1995), whereas the values of τ_{Be}^d were much shorter than those previously reported for freshwater systems: 36–1100 d (Dominik et al. 1989; Schuler et al. 1991; Steinmann et al. 1999). Although the particle reactivity of Pb is higher than that of Be in freshwater systems (e.g., Olsen et al. 1986; Benoit 1995; Chai and Urban 2004), we found slightly higher values of τ_{Pb}^d compared to τ_{Be}^d , likely due to the release of colloid-bound ^{210}Pb from the resuspension of bottom sediments. Generally, short ^7Be and ^{210}Pb residence times in most freshwater systems can be attributed to shallow depths and high SPM concentrations due to frequent sediment resuspension.

Particle residence times from ^7Be and ^{210}Pb —Particle residence times can be calculated from the following equation:

$$\tau_i^p = \text{SPM} \times \frac{H}{R_i^p} \times 365 \quad (10)$$

where τ_i^p is the residence time of particulate ^7Be or $^{210}\text{Pb}_{\text{xs}}$ (d), SPM is suspended particulate matter (g cm^{-3}), H is the height of the water column (200 cm), and R_i^p is the resuspension rate using ^7Be or $^{210}\text{Pb}_{\text{xs}}$ respectively ($\text{g cm}^{-2} \text{ yr}^{-1}$). Particle residence times ranged from 0.2 to 2.1 d (GM: 0.7 ± 1.22 d, $n = 10$) using ^7Be and from 0.5 to 8.6 d (GM: 1.6 ± 2.3 d, $n = 14$) using $^{210}\text{Pb}_{\text{xs}}$. Particle residence times in the Clinton River using ^7Be and ^{210}Pb were compared to previously reported values for lakes, which varied from 1 to 19 d and from 6 to 124 d, respectively, because there were no previously reported particle residence times for riverine systems (Benoit and Hemond 1987; Balistreri et al. 1995; Vogler et al. 1996). The particulate residence times of ^7Be and $^{210}\text{Pb}_{\text{xs}}$ were significantly shorter than the dissolved residence times, which was most likely the result of the release of colloidal-bound ^7Be and $^{210}\text{Pb}_{\text{xs}}$ into the dissolved phase during resuspension of bottom sediments. Since colloid-bound ^7Be and ^{210}Pb activities are included in the dissolved phase, the dissolved ^7Be and ^{210}Pb (measured) activities are higher than the “truly dissolved,” while the particulate ^7Be and ^{210}Pb activities are lower. The colloid-bound radionuclides also have relatively longer residence times in the water column, and hence the resuspension rates calculated using Eqs. 4 and 5 will be higher, leading to lower particle residence times.

Distribution coefficients of ^7Be and ^{210}Pb —The distribution of ^7Be and ^{210}Pb between the dissolved and particulate phases can be described by the partition coefficient (K_d):

$$K_d^i = \frac{A_i^{\text{SA}}}{A_i^d} \quad (11)$$

The K_d values of ^7Be and ^{210}Pb had a range of $0.1\text{--}2.3 \times 10^5 \text{ cm}^3 \text{ g}^{-1}$ (GM: $0.4 \times 10^5 \text{ cm}^3 \text{ g}^{-1}$, $n = 15$) and $0.1\text{--}6.5 \times 10^5 \text{ cm}^3 \text{ g}^{-1}$ (GM: $0.8 \times 10^5 \text{ cm}^3 \text{ g}^{-1}$, $n = 15$), respectively, indicating that ^{210}Pb has a slightly higher affinity for particulate matter than ^7Be in the riverine system. The K_d values of ^7Be are within the range of previously reported K_d values (1.0×10^3 and $1.0 \times 10^6 \text{ cm}^3 \text{ g}^{-1}$) found in other freshwater systems and slightly higher than K_d values of ^7Be reported for coastal seawater (6.3×10^2 to $1.0 \times 10^6 \text{ cm}^3 \text{ g}^{-1}$) (summarized in Kaste et al. 2002). The K_d values of ^{210}Pb reported in this study are an order of magnitude lower than the range reported by Chai and Urban (2004) (9.1×10^6 to $16.6 \times 10^6 \text{ cm}^3 \text{ g}^{-1}$; average: $12 \times 10^6 \text{ cm}^3 \text{ g}^{-1}$), but they are in agreement with calculated K_d values from other freshwater systems (Benoit and Hemond 1987; Balistrieri et al. 1995).

When $\log K_d$ is plotted against $\log \text{SPM}$ for ^7Be and ^{210}Pb (Fig. 7), a linear relationship with a negative slope is observed, similar to what has previously been reported (e.g., Morel and Gschwend 1987). In addition to the inverse relationship between SPM and K_d , we also found particulate fractions of ^7Be and ^{210}Pb that decreased with increasing SPM concentrations, suggesting that ^7Be and ^{210}Pb were sorbed onto or formed complexes with colloidal material. This coincided with our observations of murky water after filtration, which indicated that finer colloidal material ($<0.5 \mu\text{m}$) was present in the water. In natural systems, K_d values have been reported to be inversely proportional to SPM (e.g., O'Connor and O'Connell 1980; Honeyman and Santschi 1989; Benoit 1995), and is known as the particle concentration effect (PCE). The most widely accepted explanation of PCE proposes that metals bound to colloids are included as part of the dissolved phase (Honeyman et al. 1988; Benoit 1995). Although the PCE phenomenon has now been extensively documented in seawater, it has been rarely reported in freshwater (Hawley et al. 1986; You et al. 1989; Benoit and Rozan 1999). From the low particulate fractions and the inverse relationship found between SPM and K_d , we conclude that PCE in the Clinton River is likely due to the sorption of ^7Be and ^{210}Pb onto colloidal material. The PCE is relevant to the water quality of this and other similar freshwater systems. In particular, when particle-reactive pollutants are associated with colloidal material rather than removed onto suspended particulate matter, the mobility of these pollutants could be considerably enhanced. The mobility of such colloid-bound contaminants could affect the water quality and could be of concern in urban areas where river water is utilized for drinking.

In this first study on the partitioning of ^7Be and ^{210}Pb in a riverine system, we measured the activities of ^7Be and ^{210}Pb in sediment trap materials and particulate and dissolved phases for ~ 1 yr from May 2004 to August 2005. Based on the results presented in this study, the following significant conclusions are drawn: (1) The $^{210}\text{Pb}_{\text{xs}}$ flux in the sediment trap indicates that $\sim 98\%$ of the $^{210}\text{Pb}_{\text{xs}}$ in the trap is derived from resuspended material, which implies that resuspension events can significantly alter the mobility of particulate matter and particle-reactive contaminants in a riverine

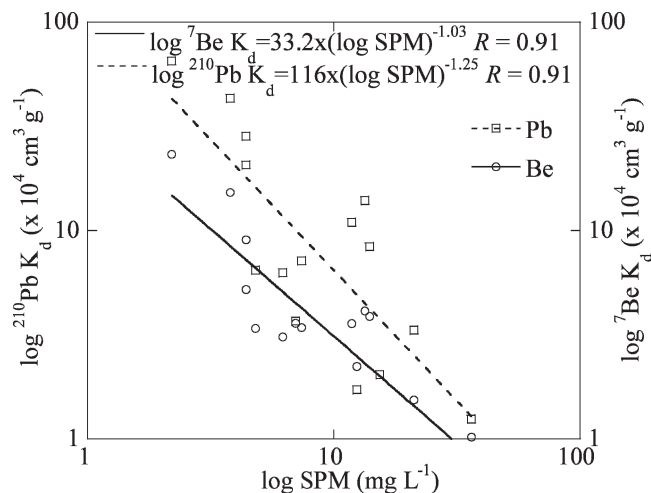


Fig. 7. The $\log \text{SPM}$ concentrations vs. $\log ^{210}\text{Pb } K_d$ and $\log ^7\text{Be } K_d$.

system. (2) The mass flux obtained in the sediment trap (GM: $8.9 \text{ g cm}^{-2} \text{ yr}^{-1}$) is about an order of magnitude higher than the long-term sediment accumulation rates (GM: $0.88 \pm 0.38 \text{ g cm}^{-2} \text{ yr}^{-1}$), which implies that the surficial sediments undergo multiple recycling before eventual burial. (3) The $^7\text{Be}:^{210}\text{Pb}_{\text{xs}}$ activity ratio of 8.3 in the long-term atmospheric deposition is significantly higher than the average values reported in the trap, suspended particulate matter, and bottom sediments. This ratio in the particulate matter is significantly altered by the extent of sediment resuspension and subsequent removal from the water column. (4) The average dissolved residence times of ^7Be and ^{210}Pb were 4.1 ± 2.7 and 9 ± 2.1 d, respectively. ^{210}Pb residence times were in the range of previously reported studies in other freshwater systems; however, ^7Be residence times were much shorter. (5) There was a strong inverse relationship between the $\log K_d$ values for both ^7Be and ^{210}Pb and $\log \text{SPM}$, indicating that there is a particle-concentration effect in the river, which we attribute to the importance of colloids in the cycling of particle-reactive species in the riverine system. Since colloids are primarily removed by coagulation and do not undergo Stokian settling, the PCE could play a major role in the mobility of particle-reactive contaminants affecting the water quality.

References

- BACON, M. P., D. W. SPENCER, AND P. G. BREWER. 1976. $^{210}\text{Pb}/^{226}\text{Ra}$ and $^{210}\text{Po}/^{210}\text{Pb}$ disequilibria in seawater and suspended particulate matter. *Earth Planet. Sci. Lett.* **32**: 277–296.
- BALISTRERI, L. S., J. W. MURRAY, AND B. PAUL. 1995. The geochemical cycling of stable Pb, ^{210}Pb , and ^{210}Po in seasonally anoxic Lake Sammamish, Washington, USA. *Geochim. Cosmochim. Acta* **59**: 4845–4861.
- BASKARAN, M., S. ASBILL, P. H. SANTSCHI, J. BROOKS, M. CHAMP, D. ADKINSON, M. R. COLMER, AND V. MAKEYEV. 1996. Pu, ^{137}Cs and excess ^{210}Pb in Russian Arctic sediments. *Earth Planet. Sci. Lett.* **140**: 243–257.

- , M. RAVICHANDRAN, AND T. S. BIANCHI. 1997. Cycling of ^7Be and ^{210}Pb in a high DOC, shallow, turbid estuary of south-east Texas. *Estuar. Coast. Shelf Sci.* **45**: 165–176.
- , AND P. H. SANTSCHI. 1993. The role of particles and colloids in the transport of radionuclides in coastal environments of Texas. *Mar. Chem.* **43**: 95–114.
- , AND ———. 2002. Particulate and dissolved ^{210}Pb activities in the shelf and slope regions of the Gulf of Mexico waters. *Cont. Shelf Res.* **22**: 1493–1510.
- BENOIT, G. 1995. Evidence of the particle concentration effect for lead and other metals in fresh waters based on ultraclean technique analyses. *Geochim. Cosmochim. Acta* **59**: 2677–2687.
- , AND H. F. HEMOND. 1987. A biogeochemical mass balance of ^{210}Po and ^{210}Pb in an oligotrophic lake with seasonally anoxic hypolimnion. *Geochim. Cosmochim. Acta* **51**: 1445–1456.
- , AND T. F. ROZAN. 1999. The influence of size distribution on the particle concentration effect and trace metal partitioning in rivers. *Geochim. Cosmochim. Acta* **63**: 113–127.
- BROECKER, W. S., A. KAUFMAN, AND R. M. TRIER. 1973. The residence time of thorium in surface sea water and its implications regarding the rate of reactive pollutants. *Earth Planet. Sci. Lett.* **20**: 35–44.
- CHAI, Y. T., AND N. R. URBAN. 2004. ^{210}Po and ^{210}Pb distributions and residence times in the nearshore region of Lake Superior. *J. Geophys. Res.* **109**: C10S07, doi:10.1029/2003JC002081.
- CHARLTON, M. N. 1983. Downflux of sediment, organic matter, and phosphorus in the Niagara River area of Lake Ontario. *J. Great Lakes Res.* **9**: 201–211.
- DOMINIK, J., C. SCHULER, AND P. H. SANTSCHI. 1989. Residence times of ^{234}Th and ^7Be in Lake Geneva. *Earth Planet. Sci. Lett.* **93**: 345–358.
- FENG, H., J. K. COCHRAN, AND D. J. HIRSCHBERG. 1999. ^{234}Th and ^7Be as tracers for the transport and dynamics of suspended particles in a partially mixed estuary. *Geochim. Cosmochim. Acta* **63**: 2487–2505.
- FITZGERALD, S. A., J. V. KLUMP, P. W. SWARZENSKI, R. A. MACKENZIE, AND K. D. RICHARDS. 2001. Beryllium-7 as a tracer of short-term sediment deposition and resuspension in the Fox River, Wisconsin. *Environ. Sci. Technol.* **35**: 300–305.
- FRANCIS, J. T., AND R. C. HAAS. 2005. Draft Clinton River assessment. Michigan Department of Natural Resources, Fisheries Division.
- HAWLEY, N., J. A. ROBBINS, AND B. J. EADIE. 1986. The partitioning of ^7Be in fresh water. *Geochim. Cosmochim. Acta* **50**: 1127–1131.
- HONEYMAN, B. D., L. S. BALISTRERI, AND J. W. MURRAY. 1988. Oceanic trace metal scavenging: The importance of particle concentration. *Deep-Sea Res. I* **35**: 227–246.
- , AND P. H. SANTSCHI. 1989. A Brownian-pumping model for oceanic trace metal scavenging evidence from Th isotopes. *J. Mar. Res.* **47**: 951–992.
- IMBODEN, D. M., AND M. STILLER. 1982. The influence of radon diffusion on the ^{210}Pb distribution in sediments. *J. Geophys. Res.* **87**: 557–565.
- KASTE, J. M., S. A. NORTON, AND C. T. HESS. 2002. Environmental chemistry of beryllium-7, p. 271–289. In S. E. Grew [ed.], *Beryllium: Mineralogy, petrology, and geochemistry*. Reviews in Mineralogy & Geochemistry, Vol. 50.
- MARVIN, C. H., E. SVERKO, M. N. CHARLTON, P. A. L. THIESSEN, AND S. PAINTER. 2004. Contaminants associated with suspended sediments in Lakes Erie and Ontario, 1997–2000. *J. Great Lakes Res.* **30**: 277–286.
- MCNEARY, D., AND M. BASKARAN. 2003. Depositional characteristics of ^7Be and ^{210}Pb in southeastern Michigan. *J. Geophys. Res.* **108**: 4210, doi: 10.1029/2002JD003021.
- MOREL, F. M. M., AND P. M. GSCHWEND. 1987. The role of colloids in the partitioning of solutes in natural waters, p. 405–422. In W. Sturm [ed.], *Aquatic surface chemistry: Chemical processes at the particle–water interface*. J. Wiley & Sons.
- O'CONNOR, D. J., AND J. P. O'CONNOLLY. 1980. The effect of concentration of adsorbing solids on the partition coefficient. *Water Res.* **14**: 1517–1523.
- OLSEN, C. R., I. L. LARSEN, P. D. LOWRY, N. H. CUTSHALL, AND M. M. NICHOLS. 1986. Geochemistry and deposition of ^7Be in river-estuarine and coastal waters. *J. Geophys. Res.* **91**: 896–908.
- ROOS, P., AND J. R. VALEUR. 2006. A sediment trap and radioisotope study to determine resuspension of particle reactive substances in the sound between Sweden and Denmark. *Cont. Shelf Res.* **26**: 474–487.
- SANTSCHI, P. H., Y.-H. LI, AND J. BELL. 1979. Natural radionuclides in the water of Narragansett Bay. *Earth Planet. Sci. Lett.* **45**: 201–213.
- SCHULER, C., E. WIELAND, P. H. SANTSCHI, M. STURM, A. LUECK, S. BOLLHALDER, J. BEER, G. BONANI, H. J. HOFMANN, M. SUTER, AND W. WOLFLI. 1991. A multitracer study of radionuclides in Lake Zurich, Switzerland: 1. Comparison of atmospheric and sedimentary fluxes of ^7Be , ^{10}Be , ^{210}Pb , ^{210}Po , and ^{137}Cs . *J. Geophys. Res.* **96**: 17051–17065.
- STEINMANN, P., T. BILLEN, J. I. LOIZEAU, AND J. DOMINIK. 1999. Beryllium-7 as a tracer to study mechanisms and rates of metal scavenging from lake surface waters. *Geochim. Cosmochim. Acta* **63**: 1621–1633.
- TRIMBLE, S. 2003. The distribution of uranium and thorium series radionuclides in the Canada Basin, Arctic Ocean. Master's thesis. Wayne State Univ.
- TRIMBLE, S. M., AND M. BASKARAN. 2005. The role of suspended particulate matter in Th-234 scavenging and Th-234-derived export fluxes of POC in the Canada Basin of the Arctic Ocean. *Mar. Chem.* **96**: 1–19.
- URBAN, N. R., X. LU, Y. T. CHAI, AND D. S. APUL. 2004. Sediment trap studies in Lake Superior: Insights into resuspension, cross-margin transport, and carbon cycling. *J. Great Lakes Res.* **30**: 147–161.
- USEPA (U. S. ENVIRONMENTAL PROTECTION AGENCY). 2006. Areas of concern (AOCs) [Internet]. U.S. Environmental Protection Agency Great Lakes National Program Office, Chicago, Illinois. [accessed 12 July 2006]. Available at: <http://www.epa.gov/glnpo/aoc/clintriv.html>
- USGS (U. S. GEOLOGICAL SURVEY). 2006. USGS 04165500 Clinton River at Moravian Drive at Mt. Clemens, MI [Internet]. U.S. Geological Survey, Lansing, Michigan. [accessed 12 July 2006]. <http://waterdata.usgs.gov/mi/nwis/uv?04165500>
- VOGLER, S., M. JUNG, AND A. MANGINI. 1996. Scavenging of ^{234}Th and ^7Be in Lake Constance. *Limnol. Oceanogr.* **41**: 1384–1393.
- YOU, C. F., T. LEE, AND Y.-H. LI. 1989. The partition of Be between soil and water. *Chem. Geol.* **77**: 105–118.

Received: 2 May 2007

Accepted: 29 February 2008

Amended: 30 April 2008